An Integrated Linear Method for Pose Estimation from Different Features

Qiang Ji[†], Mauro S. Costa[†], Robert M. Haralick[†], and Linda G. Shapiro[†,‡]

Department of Electrical Engineering[†]
Department of Computer Science and Engineering[‡]
University of Washington
Seattle WA 98195

Abstract

Existing linear solutions for the pose estimation (or exterior orientation) problem suffer from a lack of robustness and accuracy partially due to the fact that the majority of the methods utilize only one type of geometric entity and their frameworks do not allow simultaneous use of different types of features. Furthermore, the orthonormality constraints are weakly enforced or not enforced at all. We have developed a new analytic linear least-squares framework for determining pose from multiple types of geometric features. The technique utilizes correspondences between points, between lines, and between ellipse-circle pairs. The redundancy provided by different geometric features improves the robustness and accuracy of the least-squares solution. A novel way of approximately imposing orthonormality constraints on the sought rotation matrix within the linear framework is presented. Results from experimental evaluation of the new technique using both synthetic data and real images reveal its improved robustness and accuracy over existing direct methods.

1 Introduction

Pose estimation is an essential step in many machine vision and photogrammetric applications including robotics, 3D reconstruction, and mensuration. It addresses the issue of determining the position and orientation of a camera with respect to an object coordinate frame. Solutions to the pose estimation problem can be classified into linear and non-linear methods. In spite of the high susceptibility to noise, linear methods are important for computer vision problems because their computational efficiency makes automation feasible. Furthermore, direct methods offer an effective way to obtain initial estimates for use as input to non-linear, iterative methods.

Previous linear methods in pose estimation have primarily focused on using sets of 2D-3D point correspondences including the three point solution [6], the four point solutions[9, 8], and the six or more point solutions [13, 12, 5]. While point-based methods are effective and simple to implement, they are not robust and are very susceptible to noise in image coordinates, especially when the number of control points approaches the minimum required. Furthermore, finding the correspondences between the 3D scene points and 2D image pixels is also a difficult problem.

In view of these issues, other researchers [3, 10, 1, 11] have investigated the use of higher-level geometric features such as lines or curves as observed geometric entities. Analytic solutions based on high-level geometric features afford better stability and are more robust. High-level geometric features, however, may not be present in every application. Therefore, completely ignoring points while solely employing high-level geometric entities seems to be a waste of readily available information. This is one of the problems with existing solutions: they either use points or lines or conics but not a combination of features. In this paper, we describe an integrated least-squares method that determines the camera transformation matrix analytically by fusing available observed geometric information from different levels of abstraction. Specifically, we analytically solve for the external camera parameters from simultaneous use of 2D-3D correspondences between points, between lines, and between 2D ellipses and 3D circles. To our knowledge, no previous research attempts have been made in this area.

The attractiveness of our approach is that the re-

dundancy provided by different types of geometric features improves the robustness and accuracy of the least-squares solution, therefore improving the precision of the estimated parameters. To further improve the accuracy and robustness of the technique, we introduce a simple, yet effective, scheme for approximately imposing the orthonormal constraints on the rotation matrix.

This paper is organized as follows. Section 2 briefly summarizes the perspective projection geometry. Least-squares frameworks for estimating camera transformation matrix from 2D-3D point, line, and ellipse/circle correspondences are given in sections 3, 4, and 5 respectively. Section 6 discusses the integrated technique, and section 7 provides a performance characterization.

2 Perspective Projection Geometry

Let P be a 3D point and $(x\ y\ z)^t$ be the coordinates of P relative to the object coordinate frame C_o. Define the camera coordinate system C_c to have its z-axis parallel to the optical axis of the camera lens and its origin located at the perspectivity center. Let $(x_c\ y_c\ z_c)^t$ be the coordinates of P in C_c. Define C_i to be the image coordinate system, with its u-axis and v-axis parallel to the x and y axes of the camera coordinate frame, respectively. The origin of C_i is located at the principal point. Let $(u\ v)^t$ be the coordinates of P_i, the image projection of P in C_i.

Based on perspective projection theory, the projection that relates $(u\ v)^t$ on the image plane to the corresponding 3D point $(x_c\ y_c\ z_c)^t$ in the camera frame can be described by

$$\lambda(u\ v\ f)^t = (x_c\ y_c\ z_c)^t \tag{1}$$

where λ is a scalar and f is the camera focal length. Further, $(x\ y\ z)^t$ relates to $(x_c\ y_c\ z_c)^t$ by a rigid body coordinate transformation consisting of a rotation and a translation. Let a 3×3 matrix R represent the rotation and a 3×1 vector T describe the translation, then

$$(x_c\ y_c\ z_c)^t = R\ (x\ y\ z)^t + T \tag{2}$$

where T and R can be parameterized as $T = (t_x\ t_y\ t_z)$ and

$$R = (r_1\ \ r_2\ \ r_3)^t$$

in which r_i is the ith row vector of R.

R and T describe the orientation and location of the object frame relative to the camera frame respectively. Together, they are referred to as the camera transformation matrix. Combining the projection equation 1 with the rigid transformation equation 2 yields the *collinearity* equations, which describe the ideal relationship between a point on the image plane and the corresponding point in the object frame

$$u = f\frac{X'r_1 + t_x}{X'r_3 + t_z} \qquad v = f\frac{X'r_2 + t_y}{X'r_3 + t_z} \tag{3}$$

where $X = (x\ y\ z)'$. For a rigid body transformation, the rotation matrix R must be orthonormal, that is, $R^t = R^{-1}$.

3 Least-squares framework with point correspondences

Given the 3D object coordinates of a number of points and their corresponding 2D image coordinates, the coefficients of R and T can be solved for by a least-squares solution of an overdetermined system of linear equations. Specifically, the least-squares method based on point correspondences can be formulated as follows.

Let $X_n = (x_n\ y_n\ z_n)^t$, $n = 1, \ldots, K$, be the 3D coordinates of K points relative to the object frame and $U_n = (u_n\ v_n)^t$ be the observed image coordinates of these points. We can relate X_n and U_n via the collinearity equations in eq(3). Rewriting the collinearity equation yields

$$\begin{aligned} fr_1^tX_n - u_nr_3^tX_n + ft_x - u_nt_z &= 0 \\ fr_2^tX_n - v_nr_3^tX_n + ft_y - v_nt_z &= 0 \end{aligned} \tag{4}$$

We can then set up a matrix M and a vector V as follows

$$M^{2K\times 12} = \begin{pmatrix} fX_1^t & 0 & 0 & 0 & -u_1X_1^t & f & 0 & -u_1 \\ 0 & 0 & 0 & fX_1^t & -v_1X_1^t & 0 & f & -v_1 \\ \vdots & & & & & & & \\ fX_K^t & 0 & 0 & 0 & -u_K^tX_K & f & 0 & -u_K \\ 0 & 0 & 0 & fX_K^t & -v_KX_K^t & 0 & f & -v_K \end{pmatrix}$$

$$V^{12\times 1} = \begin{pmatrix} r_1^t & r_2^t & r_3^t & T^t \end{pmatrix}^t \tag{6}$$

where the collinearity matrix M is known and and vector V contains all sought rotational and translational coefficients.

4 Least-squares framework with line correspondences

Given correspondences between a set of 3D lines and their observed 2D images, we can set up a system of linear equations that involve R, T, and the coefficients for the 3D and 2D lines as follows. Let a 3D

line L in the object frame and the corresponding 2D line l in image frame be respectively represented as

$$L: \quad X = \lambda N + P \qquad l: au + bv + c = 0$$

where $X = (x\ y\ z)^t$ is a generic point on the 3D line, λ is a scalar, $N = (A, B, C)^t$ is the direction cosine of L, and $P = (P_x\ P_y\ P_z)^t$ is a known point on L.

Ideally the 3D line must lie on the projection plane formed by the center of perspectivity and the 2D image line. This leads to two constraints

$$n^t RN = 0 \qquad N^t(RP + T) = 0 \tag{7}$$

where $n = (af\ \ bf\ \ c)^t$ and f is focal length. They can be equivalently rewritten as

$$aN^t r_1 + bN^t r_2 + cN^t r_3 = 0 \tag{8}$$

$$aP^t r_1 + bP^t r_2 + cP^t r_3 + n^t T = 0 \tag{9}$$

Given a set of J line correspondences, we can set up a system of linear equations similar to those for points that involve matrix H and vector V, where V is as defined before and H is defined as follows

$$H^{2J\times 12} = \begin{pmatrix} a_1 N_1^t & b_1 N_1^t & c_1 N_1^t & 0 \\ a_1 P_1^t & b_1 P_1^t & c_1 P_1^t & n_1 \\ \vdots & & & \\ a_J N_J^t & b_J N_J^t & c_J N_J^t & 0 \\ a_J P_J^t & b_J P_J^t & c_J P_J^t & n_J \end{pmatrix} \tag{10}$$

and is called the coplanarity matrix.

5 Least-squares framework with ellipse-circle correspondences

Given the image of a circle in 3D space and the corresponding ellipse in the image, its pose relative to the camera frame can be solved for analytically. Solutions to this problem may be found in Forsyth[7], and Dhome[2]. These solutions give us the coordinates of the circle center O_c and its normal N_c relative to the camera frame Cc. If we are also given the pose of the circle in the object frame, then we can use the two poses to solve for R and T. Specifically, let $N_c = (N_{c_x}\ N_{c_y}\ N_{c_z})^t$ and $O_c = (O_{c_x}\ O_{c_y}\ O_{c_z})^t$ be the 3D circle normal and center in camera coordinates respectively. Also, let $N_o = (N_{o_x}\ N_{o_y}\ N_{o_z})^t$ and $O_o = (O_{o_x}\ O_{o_y}\ O_{o_z})^t$ be the normal and center of the same circle, but in the object coordinate system. The problem is to determine R and T from the correspondence between N_c and N_o, and between O_c and O_o. The two normals and the two centers are related by the transformation R and T as shown below

$$N_c = RN_o \qquad O_c = RO_o + T \tag{11}$$

Equivalently, we can rewrite the two equations above as follows

$$\begin{aligned} N_o^t r_1 &= N_{c_x} & O_o^t r_1 + t_x &= O_{c_x} \\ N_o^t r_2 &= N_{c_y} & O_o^t r_2 + t_y &= O_{c_y} \\ N_o^t r_3 &= N_{c_z} & O_o^t r_3 + t_z &= O_{c_z} \end{aligned}$$

Given I observed ellipses and their corresponding space circles, we can set up a system of linear equations involving matrix Q and vector k as follows

$$Q = \begin{pmatrix} N_{o_1}^t & 0 & 0 & 0 & 0 & 0 & 0 & 0 & 0 & 0 \\ 0 & 0 & 0 & N_{o_1}^t & 0 & 0 & 0 & 0 & 0 & 0 \\ 0 & 0 & 0 & 0 & 0 & 0 & N_{o_1}^t & 0 & 0 & 0 \\ O_{o_1}^t & 0 & 0 & 0 & 0 & 0 & 0 & 1 & 0 & 0 \\ 0 & 0 & 0 & O_{o_1}^t & 0 & 0 & 0 & 0 & 1 & 0 \\ 0 & 0 & 0 & 0 & 0 & 0 & O_{o_1}^t & 0 & 0 & 1 \\ \vdots & & & & & & & & & \\ N_{o_I}^t & 0 & 0 & 0 & 0 & 0 & 0 & 0 & 0 & 0 \\ 0 & 0 & 0 & N_{o_I}^t & 0 & 0 & 0 & 0 & 0 & 0 \\ 0 & 0 & 0 & 0 & 0 & 0 & N_{o_I}^t & 0 & 0 & 0 \\ O_{o_I}^t & 0 & 0 & 0 & 0 & 0 & 0 & 1 & 0 & 0 \\ 0 & 0 & 0 & O_{o_I}^t & 0 & 0 & 0 & 0 & 1 & 0 \\ 0 & 0 & 0 & 0 & 0 & 0 & O_{o_I}^t & 0 & 0 & 1 \end{pmatrix} \tag{12}$$

and

$$k = (N_{1_c}^t\ O_{1_c}^t \ldots N_{I_c}^t\ O_{I_c}^t)^t \tag{13}$$

6 The Integrated Technique

In the previous sections we have outlined the least-squares frameworks for computing the transformation matrix from point, line, and ellipse/circle pair separately. It is desirable to be able to compute camera parameters using several types of feature *simultaneously*. The problem of integrating information from points, lines, and circles is actually straightforward, given the frameworks we have outlined individually for points, lines, and circles. The problem can be stated as follows: given the 2D-3D correspondences of K points, J lines, and I ellipse/circle pairs, we want to set up a system of linear equations that involves all geometric entities. The problem can be formulated as a least-squares estimation that minimizes $||WV - b||$, where V is the unknown vector of transformation parameters as defined before, and b is a known vector defined below. W is an augmented coefficient matrix, whose rows consist of linear equations derived from points, lines, and circles. Specifically, given the M, H, and Q matrices defined in equations 5, 10, and 12, the W matrix is

$$W = (M^t \quad H^t \quad Q^t)^t \tag{14}$$

where the first $2K$ rows of W represent contributions from points, the second subsequent $2J$ rows represent contributions from lines, and the last $6I$ rows represent contributions from circles. The vector b is defined as

$$b = \begin{pmatrix} 0 & 0 & \cdots & 0 & N_{1_c}^t & O_{1_c}^t & \cdots & N_{K_c}^t & O_{K_c}^t \end{pmatrix}^t \quad (15)$$

Given W and b, the least-squares solution for V is

$$V = (W^t W)^{-1} W^t b \quad (16)$$

It can be seen that to have an overdetermined system of linear equations, we need $2K + 2J + 6I \geq 12$ observed geometric entities. This may occur with any combination of points, lines, and circles. For example, one point, one line, and one circle or two points and one circle are sufficient to solve the transformation matrix from equation 16. Any additional points or lines or circles will improve the robustness and the precision of the estimated parameters.

6.1 Approximately imposing orthonormality constraints

The least-squares solution to V described in the last section cannot guarantee the orthonormality of the resultant rotation matrix. We now introduce a simple yet effective method for approximately imposing the orthonormality constraints in a way that offers a linear solution. We want to emphasize that the technique we are about to introduce cannot guarantee a perfect rotation matrix. However our experimental study shows that it yields a matrix that is closer to a rotation matrix than those obtained using the competing methods. Given the pose of circles relative to the camera frame and the object frame, let $N_c = (N_{c_x}\ N_{c_y}\ N_{c_z})^t$ and $N_o = (N_{o_x}\ N_{o_y}\ N_{o_z})^t$ be the 3D circle normals in the camera and object frames respectively. Equation 11 depicts the relation between two normals that involves R. The relation can also be expressed in an alternative way that involves R^t as follows

$$N_o = R^t N_c \quad (17)$$

Equivalently, we can rewrite equation 17 as follows

$$\begin{aligned} N_{c_x} r_{11} + N_{c_y} r_{21} + N_{c_z} r_{31} &= N_{o_x} \\ N_{c_x} r_{12} + N_{c_y} r_{22} + N_{c_z} r_{32} &= N_{o_y} \\ N_{c_x} r_{13} + N_{c_y} r_{23} + N_{c_z} r_{33} &= N_{o_z} \end{aligned}$$

where r_{ij} is the j the element of vector r_i. Given the same set of I observed ellipses and their corresponding space circles, we can set up another system of linear equations that uses the same set of circles as in Q. Let Q' be the coefficient matrix that contains the coefficients of the set of linear equations; then Q' is

$$Q' = \begin{pmatrix} Z_{1_x} & Z_{1_y} & Z_{1_z} & 0 & 0 & 0 \\ \vdots & & & & & \\ Z_{I_x} & Z_{I_y} & Z_{I_z} & 0 & 0 & 0 \end{pmatrix} \quad (18)$$

where $Z_{i_x} = N_{i_{c_x}} I, Z_{i_y} = N_{i_{c_y}} I$, and $Z_{i_z} = N_{i_{c_z}} I$ and I is a 3×3 identity matrix.
Correspondingly, we have k' defined as

$$k' = (N_{1_o}\ 0\ 0\ 0 \ldots\ N_{I_o}\ 0\ 0\ 0)^t \quad (19)$$

To implement the constraint in the least-squares framework, we can augment matrix W in equation (14) with Q', yielding W', and augment vector b in equation (15) with k', yielding b', where W' and b' are defined as follows

$$W' = (W^t \quad Q'^t)^t \qquad b' = (b^t \quad k'^t)^t$$

Putting it all together, the solution to V can be found by minimizing $||W'V - b'||^2$ and it is given by

$$V = (W'^t W')^{-1} W'^t b' \quad (20)$$

The advantage of this technique is that the constraint is globally imposed on each entry of the rotation matrix rather than locally, and that, asymptotically, the resulting matrix converges to a rotation matrix. The resultant transformation parameters R and T are more accurate and robust due to fusing information from different sources. The resultant rotation matrix R is also very close to being orthonormal since the orthonormality constraints have been implicitly added to the system of linear equations used in the least-squares estimation.

7 Experiments

In this section, we present and discuss the results of a series of experiments aimed at characterizing the performance of the integrated linear pose estimation technique using both synthetic data and real images of industrial parts.

7.1 Experiments with synthetic data

This section consists of two parts. First, we present results from a large number of controlled experiments aimed at analyzing the effectiveness of our technique for imposing orthonormal constraints. Second, we present the results from a comparative performance study of the integrated linear technique against an existing liner technique under different noisy conditions. In the experiments with

simulation data, the 3D data (3D point coordinates, 3D surface normals, 3D line direction cosines) are generated randomly within specified ranges. 2D data are generated by projecting the 3D data onto the image plane, followed by perturbing the projected image data with iid Gaussian distributed noise of mean 0 and standard deviation σ. The average Euclidean distance between the estimated rotation (translation) vector and the ideal rotation (translation) vector is used as the performance criterion.

Figures 1 (a) and (b) plot the mean rotation and translation errors as a function of the signal to noise ratio, with and without orthonormal constraints imposed. It is clear from the two figures that imposing the orthonormal constraints improves the estimation errors for both the rotation and translation vectors. The improvement is especially significant when the SNR is low. To further study the effectiveness of the technique for imposing constraints, we studied its performance under different numbers of pairs of ellipse/circle correspondences. The results are plotted in Figure 2 (a) and (b), which gives the average rotation and translation errors as a function of the number of ellipse/circle pairs used, with and without constraints imposed. The two figures again show that imposing orthonormal constraints leads to an improvement in estimation errors. The technique for imposing constraints is most effective when fewer ellipse/circle pairs are used.

To compare the integrated linear technique with an existing linear technique, we studied its performance against that of Faugeras [4]. The results are given in Figures 3 (a) and (b), which plot the mean rotation and translation vector errors as a function of the SNR respectively. The curve for Faugeras's method was obtained using 10 points; while the curve for the integrated technique was generated using a combination of one point, one line, and three circles. The two figures clearly show the superiority of the new integrated technique over Faugeras' linear technique, especially for the translation errors. To further compare the sensitivity of the two techniques to viewing parameters, we changed the position parameters of the camera by increasing z. Figures 4 (a) and (b) plot the mean rotation and translation vector errors respectively as a function of SNR under the new camera position.

While increasing z causes an increase in the estimation errors for both techniques, its impact on Faugeras' technique is more serious. This leads to a much more noticeable performance difference between the two linear techniques. Faugeras's technique is apparently numerically unstable to viewing parameters. The fact that the integrated technique using only five geometric entities (1 line, 1 point, and 3 circles) still outperforms Faugeras' technique, which uses 10 points, demonstrates the power of combining features on different levels of abstraction.

7.2 Performance characterization with real images

This section presents results obtained using real images of industrial parts. First, we visually assess the performance of the integrated technique against existing techniques that use only one type of geometric entity. The performance of the proposed technique is judged by visual inspection of the alignment between the image of a part and the reprojected outline of the part using the estimated transformation matrix. Figure 5 illustrates the results obtained using the combination of features: one point, two lines, and one circle. The result for the pose computation using Faugeras[5] technique with six points is given in Figure 6 (a). The algorithm of Forsyth [7] for the pose-from-circle computation was augmented to handle non-rotationally symmetric objects. The results of this augmented algorithm using the single ellipse/circle correspondence are shown in Figure 6 (b).

Visual inspection of the above figures clearly shows the superiority of the integrated technique to the linear techniques that use only one type of geometric entity. Notice that due to the localized concentration of detectable feature points and the physical distance between the circle and these points, the poses computed align well only in the areas where the features used are located. Specifically, the result in Figure 6 (a) shows a good alignment in the upper portion of the object where the circle is located and a poor alignment in the lower part (as indicated by the arrow). On the other hand, the result in Figure 6 (b) shows good alignment only at the lower part of the object where the concentration of detectable feature points is located and a poor alignment on the upper part of the object (as indicated by the arrow). To further validate our technique, we tested it on over fifty images of industrial parts and achieved similar results.

Second, to compare the performance quantitatively, we compute the number of iterations required for the iterative procedure to converge using as initial guesses the results from the three linear methods illustrated in Figures 5 and 6. The results reveal that the technique with only points and only circles need 4 and 6 iterations respectively to converge, while the technique using both points and cir-

cles together needs only one iteration to converge. This shows that combining different features may yield a transformation matrix very close to the one obtained from the iterative procedure. This echoes the conclusion from visual inspection: the new technique offers better estimation accuracy.

8 Conclusions

In this paper, we present an integrated technique for the pose estimation problem. The main contributions of this research are the linear framework for fusing information available from different geometric entities and the technique for approximately imposing the orthonormality constraints. An experimental evaluation using both synthetic data and real images shows the effectiveness of our technique for imposing orthonormality constraints and improving estimation errors. The technique is especially effective when the SNR is low. The performance study also revealed superiority of the integrated technique to a competing linear technique in terms of robustness and accuracy. The new technique proposed in this paper is ideal for applications such as industrial automation where robustness, accuracy, computational efficiency, and speed are needed.

References

[1] Shu-Yuan Chen and Wen-Hsiang Tsai. Systematic approach to analytic determination of camera parameters by line features. *Pattern Recognition*, 23(8):859–897, 1990.

[2] M. D. Dhome and et al. Spatial localization of modeled objects of revolution in monocular perspective vision. In *First European Conference on Computer Vision*, 1989.

[3] Tomio Echigo. Camera calibration technique using three sets of parallel lines. *Machine Vision and Applications*, 3(3):159–167, 1990.

[4] O. D. Faugeras. *Three Dimensional Computer Vision: A Geometric Viewpoint.* MIT Press, 1993.

[5] Olivier Faugeras. *Three-Dimensional Computer Vision.* The MIT Press, Cambirdge, Massachusetts, 1993.

[6] M. A. Fischler and R. C. Bolles. Random sample consensus: A paradigm for model fitting with applications to image analysis and automated cartography. *Communications of the ACM*, 24(6):381–395, 1981.

[7] D. Forsyth, J. L. Mundy, A. Zisserman, and et al. Invariant descriptors for 3d object recognition and pose. *IEEE Trans. on Pattern Analysis and Machine Intelligence*, 13(10):971–991, 1991.

[8] R. J. Holt and A. N. Netravali. Camera calibration problem: some new results. *Computer Vision, Graphics, and Image Processing*, 54(3):368–383, 1991.

[9] Y. Hung, P. S. Yeh, and D. Harwood. Passive ranging to known planar point sets. *Proceedings of IEEE Int. Conf. on Robotics and Automation*, pages 80–85, 1985.

[10] Yubcai Liu, T.S. Huang, and O. D. Faugeras. Determination of camera locations from 2d to 3d line and point correspondence. *IEEE Trans. on Pattern Analysis and Machine Intelligence*, 12(1):28–37, 1990.

[11] C. A. Rothwell, A. Zisserman, C. I. Marinos, D.A. Forsyth, and J. L. Mundy. Relative motion and pose from arbitrary plane curves. *Image and Vision Computing*, 10(4):251–262, 1992.

[12] Ivan E. Sutherland. Three-dimensional data input by tablet. *Proceedings of the IEEE*, 62(4):453–461, 1974.

[13] R. Tsai. A versatile camera calibration technique for high-accuracy 3d machine vision metrology using off-the-shelf tv cameras and lens. *IEEE Journal of Robotics and Automation*, 3:223–244, 1987.

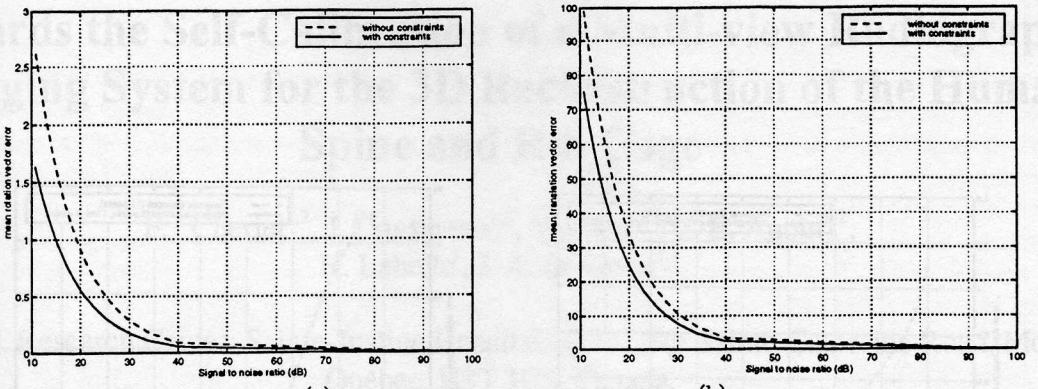

(a) (b)

Figure 1: (a) Average rotation vector error (b) Average translation vector error versus SNR.

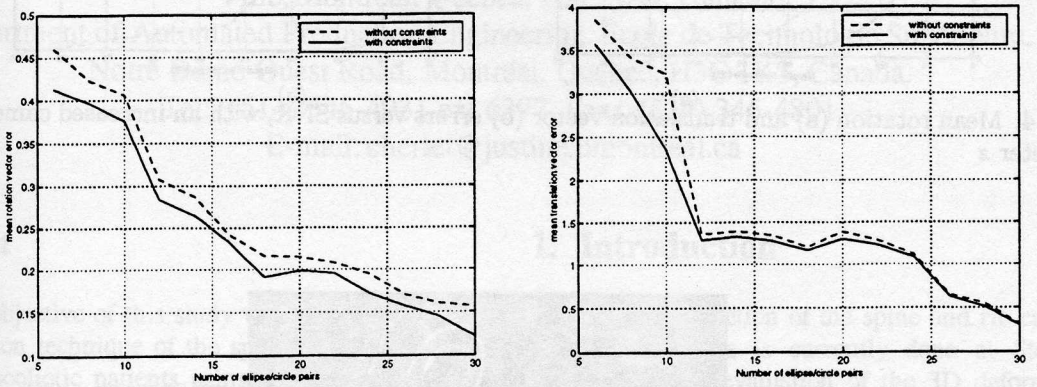

(a) (b)

Figure 2: (a) Average rotation vector error, and (b) Average translation vector error versus number of ellipse/circle pairs.

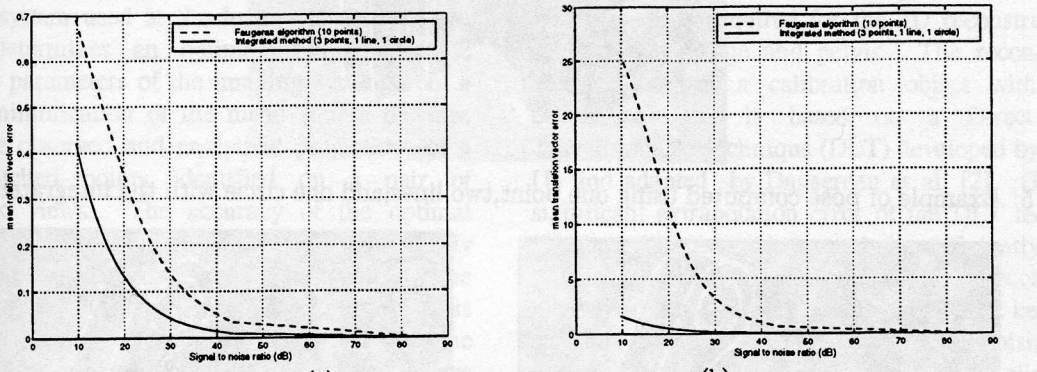

(a) (b)

Figure 3: Mean rotation (a) and translation vector (b) errors versus SNR.

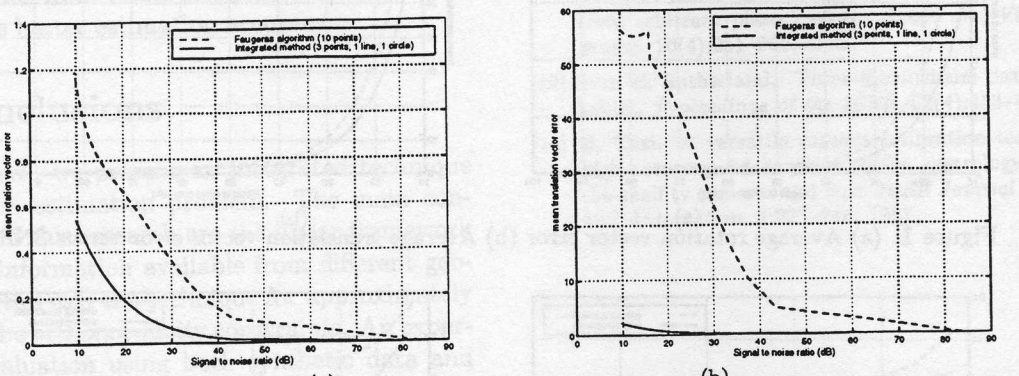

(a) (b)

Figure 4: Mean rotation (a) and translation vector (b) errors versus SNR, with an increased camera position parameter z

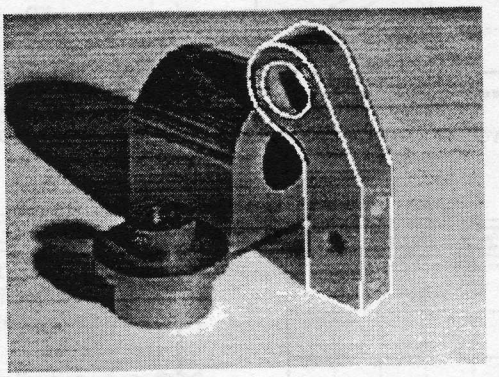

Figure 5: Example of pose computed using one point,two lines,and one circle with the integrated technique.

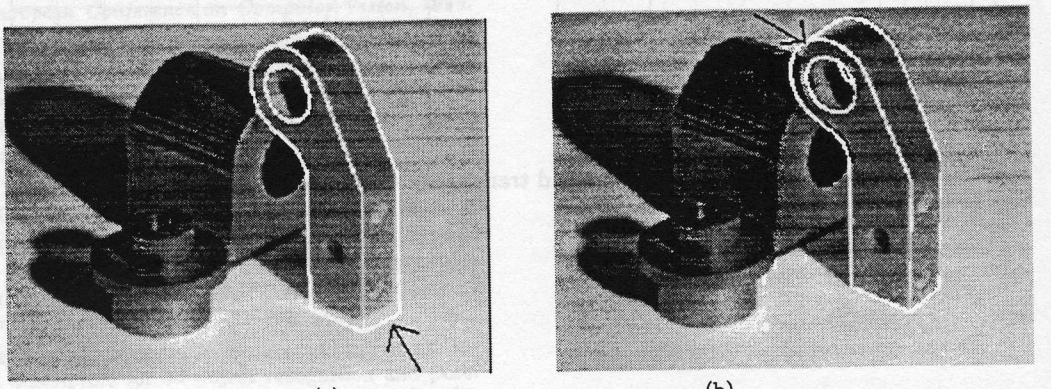

(a) (b)

Figure 6: The pose computed using (a) a single circle/ellipse pair and (b) six points only.